TOFlow: Learning-Based Isotropic Reconstruction and Flow Mapping from Multi-Orientation TOF-MRA

Daria Hasin[1,2], Amit H. Bermano[3], Udi Sadeh Gonik[4], Orna Aizenstein[4], and Dafna Ben Bashat[1,2]

[1] Sagol Brain Institute, Tel Aviv Sourasky Medical Center, Tel Aviv, Israel
[2] Sagol School of Neuroscience, Tel Aviv University, Tel Aviv, Israel
[3] The Blavatnik School of Computer Science, Tel Aviv University, Tel Aviv, Israel
[4] Department of Radiology, Tel Aviv Sourasky Medical Center, Tel Aviv, Israel
dafnab@tlvmc.gov.il

Abstract. Accurate assessment of vascular pathologies, such as aneurysms, requires reliable visualization of the cerebral vasculature. Time-of-Flight MR angiography (TOF-MRA) is a standard MRI technique for non-contrast, radiation-free imaging of the intracranial vasculature. However, anisotropic resolution and orientation-dependent sensitivity limit depiction of small or in-plane vessels, especially with slow flow. While TOF-MRA is primarily structural, 4D Flow MRI provides flow measurements, though long, gated, low-resolution acquisitions restrict brain coverage and limit routine clinical use in neuroimaging. In this work, we propose TOFlow, a neural reconstruction framework that fuses multi-orientation TOF-MRA acquisitions to address anisotropy and orientation-dependent signal effects and enable flow-related information estimation. The method integrates multi-view scans and incorporates a streamline-consistency constraint to resolve directional ambiguity and enforce coherent flow patterns. Experimental results demonstrate that TOFlow produces high-quality isotropic reconstructions while preserving signal-to-noise characteristics and enabling estimation of relative flow patterns and directionality. These findings are supported by quantitative image quality metrics and qualitative radiologists' evaluation. Voxel-wise flow-direction and relative-intensity maps demonstrate improved directional coherence relative to 4D Flow MRI, as quantified by vessel-alignment and velocity-profile metrics. These results support TOFlow as a TOF-MRA-based framework for isotropic reconstruction and flow mapping.

Keywords: TOF-MRA · Implicit Neural Representation · 3D Reconstruction · Cerebral Vasculature

1 Introduction

Accurate visualization of the vascular network is important for the diagnosis and longitudinal follow-up of cerebrovascular diseases, such as intracranial

aneurysms, arterial stenosis or occlusion, and arteriovenous malformations [7]. In current clinical practice, Time-of-Flight Magnetic Resonance Angiography (TOF-MRA) is a widely used non-invasive modality for neurovascular imaging due to high its strong vessel-to-background contrast and independence from contrast agents [6]. TOF-MRA can be acquired using either 3D or 2D sequences. While 3D TOF is the standard technique for intracranial angiography due to its high spatial resolution, 2D TOF is used in clinical practice when greater sensitivity to slow flow is needed, such as in distal vessels or venography [10]. Despite its widespread clinical use, standard 3D TOF-MRA remains limited by anisotropic resolution and physics-based sensitivity to blood-flow orientation relative to the imaging plane. These technical limitations often lead to signal loss in vessels with in-plane or slow-flow components, preventing the consistent depiction of small or tortuous vessels [13].

4D Flow MRI is an imaging technique that provides time-resolved, 3D visualization of blood flow and enables quantitative assessment of vascular hemodynamics. However, its application in neurovascular imaging is constrained by long acquisition times and relatively low spatial resolution, which limit its ability to resolve fine intracranial vessels [8].

Developments in Implicit Neural Representations (INRs), such as Neural Radiance Fields (NeRFs) [9], have offered a paradigm shift in volumetric reconstruction by modeling volumes as continuous, resolution-agnostic functions. The NeSVoR (Neural Slice-to-Volume Reconstruction) framework [14] has demonstrated the potential of these models to integrate heterogeneous slice data into cohesive volumes, particularly in motion-prone scenarios like fetal MRI. However, the application of INRs to TOF-MRA has not been previously explored, and standard formulations are designed for scalar intensity fields rather than the vector-valued representations, where signal intensity varies across different orientations due to flow-dependent effects.

In this paper, we introduce TOFlow, a neural reconstruction framework for isotropic super-resolution and voxel-wise blood-flow mapping in cerebral TOF-MRA. Our main contributions are:

1. Leveraging multi-orientation TOF-MRA acquisitions and the orientation-dependent nature of the TOF signal for isotropic reconstruction and flow-related estimation.
2. Extending the NeSVoR framework to learn voxel-wise vector-valued representations of flow magnitude and direction from TOF-MRA data.
3. Introducing a streamline-consistency loss to resolve directional ambiguity and enforce coherent vessel-aligned flow estimation.

Together, these contributions enable high-resolution reconstruction and coherent flow-direction estimation from clinical TOF-MRA without dedicated flow imaging.

2 Methodology

TOFlow pipeline is illustrated in Fig. 1. The framework reconstructs an isotropic volume and estimates voxel-wise flow direction from multi-orientation TOF-MRA acquisitions.

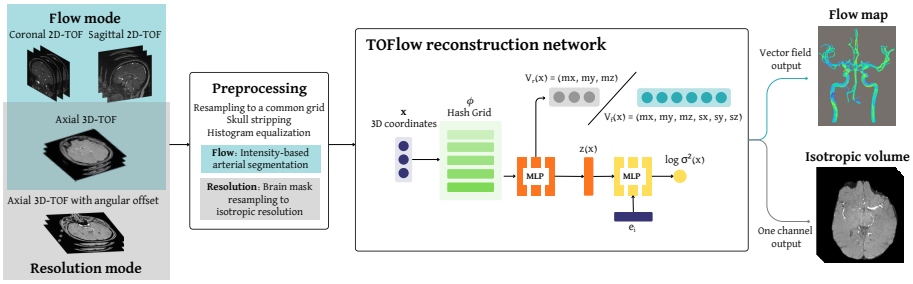

Fig. 1. TOFlow pipeline. Multi-orientation TOF-MRA is used to reconstruct an isotropic volume and estimate voxel-wise flow. Gray denotes resolution mode, and light blue denotes flow mode.

2.1 Multi-Orientation Acquisition and Preprocessing

Multi-orientation TOF-MRA acquisitions were obtained to exploit the orientation-dependent nature of the TOF signal. For isotropic reconstruction, two axial 3D TOF-MRA scans were acquired, including a standard clinical scan and an additional scan rotated by approximately 23°. For flow mapping, in addition to the axial 3D TOF-MRA scan, two 2D TOF-MRA acquisitions were obtained in the coronal and sagittal planes.

All scans were resampled into the coordinate system of the axial 3D TOF reference volume using rigid transformations estimated with ANTsPy [1], bringing the volumes into a shared coordinate space while preserving acquisition geometry. Skull stripping was performed using SynthStrip [4] and for isotropic reconstruction, the resulting brain mask was resampled to the target isotropic resolution and used to define the coordinates sampled during reconstruction. Histogram equalization was applied using SimpleITK [15]. For flow-mapping, an additional intensity-based vessel segmentation was performed in 3D Slicer [2] to generate masks that guided sampling of the reconstructed flow field.

2.2 Network Architecture

As shown in Fig. 1, the core of TOFlow is an implicit neural representation based on a modified NeSVoR model [14], where spatial coordinates $\mathbf{x} \in \mathbb{R}^3$ are encoded using multi-resolution hash-grid encoding $\phi(\mathbf{x})$ and processed by a multi-layer perceptron (MLP). An auxiliary uncertainty head predicts the log-variance

$\log(\sigma^2(\mathbf{x}))$ for per-point uncertainty weighting, utilizing acquisition-specific slice embeddings. The network architecture employs task-specific heads to parameterize the output $V(\mathbf{x})$. TOFlow operates in two modes: **resolution mode** for isotropic reconstruction and **flow mode** for estimating voxel-wise flow direction. In resolution mode, the network predicts axis-specific magnitude components (m_x, m_y, m_z) constrained by a softplus activation. The final reconstructed isotropic volume is obtained by sampling the m_z component, corresponding to the primary axial acquisition direction. In flow mode, the network predicts magnitude (m_x, m_y, m_z) and direction (s_x, s_y, s_z) components. Direction values are discretized to ± 1 to represent signed flow orientation, and a straight-through estimator is used to enable gradient propagation during training. The final signed flow vector is computed as their element-wise product, representing 3D flow direction and relative magnitude.

2.3 Loss Functions

The training loss builds on the formulation of NeSVoR [14], including Gaussian negative log-likelihood data fidelity, spatial regularization, and uncertainty regularization. The data fidelity term is modified to explicitly account for orientation-dependent TOF signal formation. Instead of directly comparing predicted and observed intensities, the acquired slice intensity is compared to a synthesized signal obtained by projecting the predicted magnitude vector onto the corresponding slice normal. For the resolution branch, a foreground separation loss using binary cross-entropy is applied to the projected signal to encourage sharper contrast between the vasculature and the background.

Streamline Consistency Loss. To resolve the directional sign ambiguity inherent in TOF-MRA, the flow-mapping pipeline introduces a novel Streamline-Consistency Loss. This loss initializes seed points within the vessel mask and advances them in the predicted direction for N steps to trace streamlines. Formally, the loss is defined as

$$\mathcal{L}_{\text{streamline}} = \frac{1}{N} \sum_{t=1}^{N} (1 - \cos(\theta_t)) + \lambda_{\text{exit}} \left(1 - \frac{1}{T} \sum_{t=1}^{N} M(t) \right) \tag{1}$$

The loss consists of two components. The first penalizes the angle θ_t between consecutive steps, enforcing directional coherence along vessels. The second applies an early-exit penalty using a soft vessel indicator $M(t) \in [0, 1]$ obtained by bilinear sampling of the vessel mask, where premature exit results in a larger penalty weighted by λ_{exit}. Here, T denotes the maximum number of tracing steps and N the number of valid steps. In our experiments, λ_{exit} was set to 0.5, and the number of tracing steps was gradually increased from 20 to 30 during training, with step size 0.1 and early-exit penalty weight 0.5.

3 Experimental Results

3.1 Dataset

Six subjects were included for isotropic reconstruction evaluation, including five healthy controls and one patient with an intracranial aneurysm. Three of these subjects had reference high-resolution isotropic 3D TOF-MRA available for quantitative comparison. Flow-mapping evaluation was performed on six subjects, with partial overlap between the cohorts, including one subject with reference 4D Flow MRI. All scans were acquired on 3T Siemens Prisma or Cima.X Fit systems. The protocol for isotropic reconstruction included 3D axial TOF-MRA with 0.3–0.4 mm in-plane resolution and 0.6–0.7 mm slice thickness. The flow protocol combined one 3D TOF axial and two orthogonal 2D TOF acquisitions with voxel size of approximately $1 \times 1 \times 1.5$ mm^3. Reference high-resolution isotropic 3D TOF-MRA was acquired at 0.3 mm isotropic resolution. In one subject, reference 4D Flow MRI with cardiac gating was additionally acquired for flow comparison.

This study was approved by the local ethics committee of Tel Aviv Sourasky Medical Center (Helsinki Committee, Approval No. 0038-08).

3.2 Implementation Details

The implicit neural representation was optimized separately for each subject and reconstruction task, learning a continuous representation directly from the acquired multi-orientation scans. Reconstruction required approximately 13 minutes per subject for each reconstruction task. TOFlow was implemented in PyTorch and trained on a Linux workstation with an NVIDIA RTX 4060 Ti GPU with 16 GB memory. The model was optimized using AdamW with initial learning rate 5×10^{-3}, batch size 2,048 and 8,000 iterations. The MLP network consisted of one hidden layer with 64 neurons and ReLU activation.

3.3 Evaluation Metrics

Reconstruction quality was evaluated using PSNR, SSIM, NRMSE, and NCC, and perceptual quality using FID [3] and VIF [12]. Global SNR was estimated using a three-component Gaussian mixture model representing cerebrospinal fluid, brain tissue, and vasculature. Flow mapping accuracy was quantified using magnitude-weighted Flow Jet Angle (FJA) and normalized Flow Displacement (FD), computed on vessel cross-sections orthogonal to the centerline [11]. Qualitative evaluation was performed in a blinded manner by a neuroradiologist and an interventional radiologist using a five-point Likert scale. Flow maps were additionally reviewed for anatomical plausibility. This radiological evaluation was conducted on a research workstation display rather than a clinical diagnostic monitor.

3.4 Isotropic Reconstruction Results

Quantitative analysis. We quantitatively compared the proposed TOFlow reconstruction with NeSVoR reconstruction adapted for high-resolution TOF-MRA and with a classical slice-to-volume reconstruction using SVRTK [5]. Results are summarized in Table 1.

Table 1. Quantitative comparison between SVRTK, NeSVoR, and the proposed TOFlow method. Values are mean ± standard deviation.

	Image Quality Metrics				Perceptual Metrics	
Method	PSNR ↑	SSIM ↑	NRMSE ↓	NCC ↑	VIF ↑	FID ↓
SVRTK	37.55 ± 1.94	**0.98 ± 0.01**	0.013 ± 0.002	0.93 ± 0.02	0.60 ± 0.07	2.89 ± 0.78
NeSVoR	33.02 ± 2.34	0.26 ± 0.03	0.02 ± 0.01	**0.97 ± 0.01**	0.39 ± 0.05	5.52 ± 1.58
TOFlow	**39.48 ± 1.67**	0.97 ± 0.01	**0.011 ± 0.002**	0.95 ± 0.01	**0.67 ± 0.06**	**2.89 ± 0.85**

TOFlow demonstrated improved reconstruction fidelity and perceptual quality compared to NeSVoR and SVRTK, achieving the best overall performance across most quantitative and perceptual metrics. Visual comparison in Fig. 2 further illustrates improved preservation of fine vascular structures.

SNR analysis. In three subjects with available isotropic high-resolution TOF-MRA acquisitions, TOFlow achieved higher SNR than the acquired isotropic scan, reaching 14.96 ± 0.27 compared to 10.73 ± 0.66, corresponding to an SNR ratio of 1.40 ± 0.11, which closely matches the theoretical $\sqrt{2}$ improvement expected from combining two independent acquisitions. Across all six subjects, reconstructed volumes achieved an SNR of 13.11 ± 2.64 compared to 12.42 ± 2.00 in the original acquisitions, indicating that signal quality was preserved despite the increased spatial resolution.

Radiologist evaluation. Qualitative assessment focused on diagnostic interpretability, depiction of small and distal vessels, image noise and artifacts, and overall clinical usability. All TOFlow reconstructions were considered diagnostically interpretable by both readers, and a confident clinical report could be issued in all cases. The neuroradiologist noted improved visualization of distal and small-caliber vessels in several reconstructions. Similarly, the interventional radiologist frequently rated the reconstructed volumes higher in terms of noise and artifacts, indicating cleaner appearance and improved signal-to-noise characteristics in those cases. At the same time, both radiologists noted reconstruction-related artifacts in some subjects, including pixelated or artificial appearance, which affected subjective vessel sharpness. Despite these limitations, clinically relevant vascular anatomy was preserved, and improved depiction of small vessels was observed in several cases.

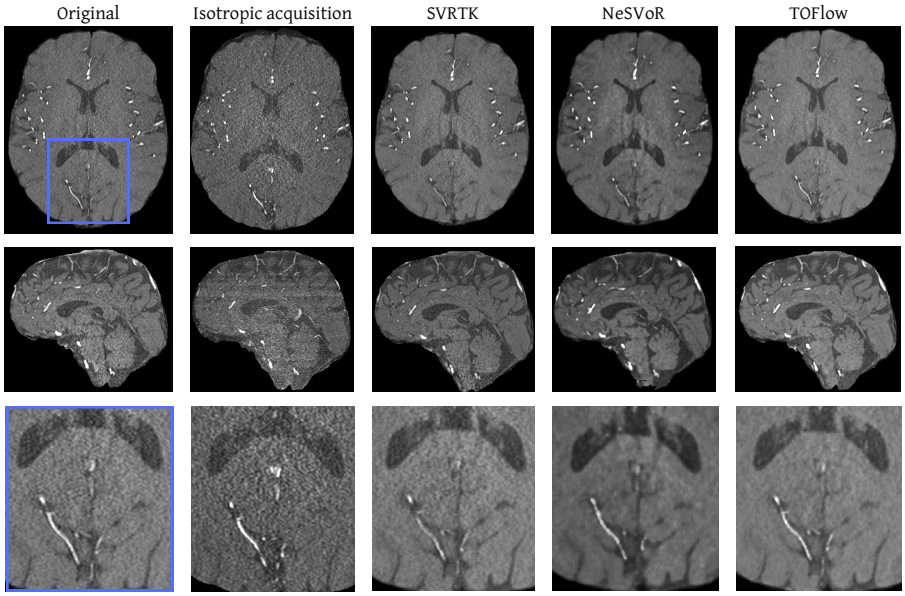

Fig. 2. Visual comparison of 3D-TOF volumes. The original axial TOF-MRA is shown as reference, alongside the direct isotropic acquisition and isotropic reconstructions obtained using SVRTK, NeSVoR, and the proposed TOFlow method.

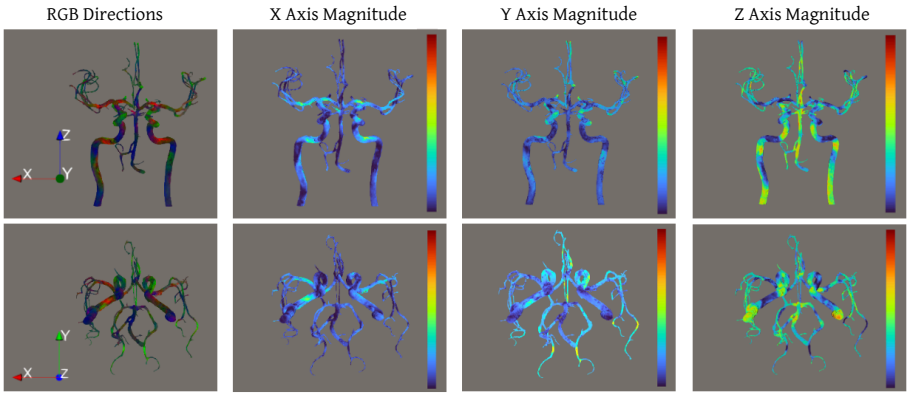

Fig. 3. Visualization of the reconstructed vascular flow direction field. The left column shows RGB-encoded flow directions, where red, green, and blue correspond to the x, y, and z direction components, respectively. The remaining columns show the magnitude of each directional component separately.

3.5 Flow Mapping Results

Comparison with 4D Flow MRI Quantitative comparison with 4D Flow MRI was performed in one subject with available reference data and was used as an exploratory proof-of-concept comparison. TOFlow achieved lower FJA and FD values compared to 4D Flow MRI, indicating closer alignment of flow vectors with vessel centerlines and a more centered velocity distribution. As shown in Fig. 4, the distributions for TOFlow are shifted toward lower values for both metrics, reflecting improved directional coherence and physiologically consistent flow patterns.

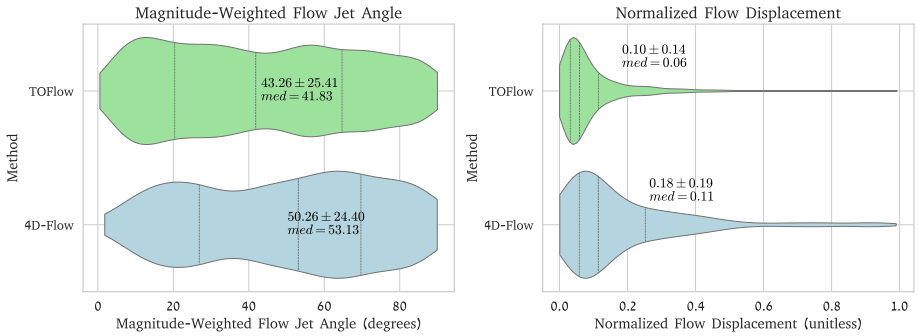

Fig. 4. TOFlow and 4D Flow MRI comparison in one subject.

Streamline-consistency loss ablation study The contribution of the streamline-consistency loss was evaluated by comparing models trained with and without this loss term. The model with streamline-consistency loss achieved a lower subject-averaged FJA of 44.64±2.37° compared to 56.67±0.77° for the model trained without the loss, demonstrating that the streamline-consistency loss improves directional consistency. FD values were similar between configurations (0.14±0.01 without the loss vs. 0.15±0.01 with the loss), indicating that the streamline-consistency loss improves directional consistency while preserving the overall velocity distribution.

Radiologist evaluation. Qualitative assessment focused on the anatomical plausibility of the predicted flow patterns and directional coherence along vessels. Flow visualizations generated by TOFlow were considered visually interpretable by the neuroradiologist, with coherent and physiologically plausible directional organization and clear depiction of relative flow differences across vessels. The visualizations were regarded as promising for illustrating vascular flow behavior and exploring flow-related alterations. The radiologist emphasized

that systematic evaluation across larger cohorts, including direct comparison between healthy and pathological cases, together with quantitative analysis, will be necessary to establish clinically meaningful conclusions and determine potential clinical utility.

4 Conclusion

We presented TOFlow, a neural field–based framework for isotropic reconstruction and directional flow mapping from multi-orientation TOF-MRA acquisitions. By integrating complementary information across scan orientations, TOFlow enables reconstruction of high-resolution isotropic volumes and estimation of voxel-wise flow direction and relative velocity without dedicated flow imaging. Quantitative and qualitative evaluation demonstrated improved reconstruction quality compared to direct isotropic acquisitions and showed that the predicted flow patterns are anatomically plausible and clinically interpretable. Future work will focus on validation in larger and more diverse cohorts, quantitative comparison with 4D Flow MRI in a larger number of subjects, optimization of acquisition protocols and reconstruction efficiency, and further development of the framework toward improved flow quantification and evaluation of its potential clinical utility for assessing vascular abnormalities.

Disclosure of Interests. The authors have no competing interests to declare that are relevant to the content of this article.

References

1. Avants, B.B., Tustison, N.J., Song, G., Cook, P.A., Klein, A., Gee, J.C.: A reproducible evaluation of ANTs similarity metric performance in brain image registration. NeuroImage **54**(3), 2033–2044 (Feb 2011). https://doi.org/10.1016/j.neuroimage.2010.09.025, https://www.sciencedirect.com/science/article/pii/S1053811910012061
2. Fedorov, A., Beichel, R., Kalpathy-Cramer, J., Finet, J., Fillion-Robin, J.C., Pujol, S., Bauer, C., Jennings, D., Fennessy, F., Sonka, M., Buatti, J., Aylward, S., Miller, J.V., Pieper, S., Kikinis, R.: 3D Slicer as an image computing platform for the Quantitative Imaging Network. Magnetic Resonance Imaging **30**(9), 1323–1341 (Nov 2012). https://doi.org/10.1016/j.mri.2012.05.001, https://linkinghub.elsevier.com/retrieve/pii/S0730725X12001816
3. Heusel, M., Ramsauer, H., Unterthiner, T., Nessler, B., Hochreiter, S.: GANs Trained by a Two Time-Scale Update Rule Converge to a Local Nash Equilibrium (Jan 2018). https://doi.org/10.48550/arXiv.1706.08500, http://arxiv.org/abs/1706.08500, arXiv:1706.08500 [cs]
4. Hoopes, A., Mora, J.S., Dalca, A.V., Fischl, B., Hoffmann, M.: SynthStrip: skull-stripping for any brain image. NeuroImage **260**, 119474 (Oct 2022). https://doi.org/10.1016/j.neuroimage.2022.119474, https://linkinghub.elsevier.com/retrieve/pii/S1053811922005900

5. Kuklisova-Murgasova, M., Quaghebeur, G., Rutherford, M.A., Hajnal, J.V., Schnabel, J.A.: Reconstruction of fetal brain MRI with intensity matching and complete outlier removal. Medical Image Analysis **16**(8), 1550–1564 (Dec 2012). https://doi.org/10.1016/j.media.2012.07.004, https://linkinghub.elsevier.com/retrieve/pii/S1361841512000965
6. Kuo, A.H., Nagpal, P., Ghoshhajra, B.B., Hedgire, S.S.: Vascular magnetic resonance angiography techniques. Cardiovascular Diagnosis and Therapy **9**(S1), S28–S36 (Aug 2019). https://doi.org/10.21037/cdt.2019.06.07, http://cdt.amegroups.com/article/view/27089/24959
7. Li, X., Su, F., Yuan, Q., Chen, Y., Liu, C.Y., Fan, Y.: Advances in differential diagnosis of cerebrovascular diseases in magnetic resonance imaging: a narrative review. Quantitative Imaging in Medicine and Surgery **13**(4), 2712–2734 (Apr 2023). https://doi.org/10.21037/qims-22-750, https://qims.amegroups.com/article/view/110343/html
8. Markl, M., Frydrychowicz, A., Kozerke, S., Hope, M., Wieben, O.: 4D flow MRI. Journal of Magnetic Resonance Imaging **36**(5), 1015–1036 (2012). https://doi.org/10.1002/jmri.23632, https://onlinelibrary.wiley.com/doi/abs/10.1002/jmri.23632, _eprint: https://onlinelibrary.wiley.com/doi/pdf/10.1002/jmri.23632
9. Mildenhall, B., Srinivasan, P.P., Tancik, M., Barron, J.T., Ramamoorthi, R., Ng, R.: NeRF: Representing Scenes as Neural Radiance Fields for View Synthesis (Aug 2020), http://arxiv.org/abs/2003.08934, arXiv:2003.08934 [cs]
10. Ozsarlak, O., Van Goethem, J.W., Maes, M., Parizel, P.M.: MR angiography of the intracranial vessels: technical aspects and clinical applications. Neuroradiology **46**(12), 955–972 (Dec 2004). https://doi.org/10.1007/s00234-004-1297-9, http://link.springer.com/10.1007/s00234-004-1297-9
11. Ramaekers, M.J.F.G., Westenberg, J.J.M., Adriaans, B.P., Nijssen, E.C., Wildberger, J.E., Lamb, H.J., Schalla, S.: A clinician's guide to understanding aortic 4D flow MRI. Insights into Imaging **14**(1), 114 (Jul 2023). https://doi.org/10.1186/s13244-023-01458-x, https://insightsimaging.springeropen.com/articles/10.1186/s13244-023-01458-x
12. Sheikh, H.R., Bovik, A.C.: Image Information and Visual Quality
13. Shin, T.: Principles of Magnetic Resonance Angiography Techniques. Investigative Magnetic Resonance Imaging **25**(4), 209–217 (Dec 2021). https://doi.org/10.13104/imri.2021.25.4.209, https://doi.org/10.13104/imri.2021.25.4.209
14. Xu, J., Moyer, D., Gagoski, B., Iglesias, J.E., Grant, P.E., Golland, P., Adalsteinsson, E.: NeSVoR: Implicit Neural Representation for Slice-to-Volume Reconstruction in MRI. preprint (Nov 2022). https://doi.org/10.36227/techrxiv.21398868.v1, https://www.techrxiv.org/doi/full/10.36227/techrxiv.21398868.v1
15. Yaniv, Z., Lowekamp, B.C., Johnson, H.J., Beare, R.: SimpleITK Image-Analysis Notebooks: a Collaborative Environment for Education and Reproducible Research. Journal of Digital Imaging **31**(3), 290–303 (Jun 2018). https://doi.org/10.1007/s10278-017-0037-8, https://doi.org/10.1007/s10278-017-0037-8